Impact assessment of FACTS and VSC-HVDC for damping power oscillations based on location and control strategy

Aziz Un Nur Ibn Saif, Md. Masum Howlader, Md. Tareq Ul Islam

Abstract— This paper examines the impact of SVC, TCSC and VSC-HVDC on stability of electric power system. The stability study includes both static voltage stability and power oscillation for different kinds of control strategies based on linear and nonlinear theory. Dynamic responses have been investigated by injecting different disturbances into the test power system. For each device the efficiency of several Power Oscillation Damping (POD) strategies have been compared. Two criteria is selected to define the most appropriate coupled POD-devices: its specificity and efficiency. A brand view of the time response of each couple after two selected disturbances is provided at the end of the paper.

Index Terms— **CLF, FACTS, POD, SVC, TCSC, VSC-HVDC, Inter-area mode**
.

1 INTRODUCTION

An electrical network [1] must be designed to maintain desired performances under disturbances and recent blackouts menifest the need of application of power electronic devices in the network [2]. The performance of our interest here is the ability of the system to prevent the generator from oscillating against each other such as it happens sometimes in reality [3] and to control the bus voltages. This performance could be enhanced by building new lines or adding bank capacitors. Our devices based on power electronic technologies can avoid heavy investments (new lines) while performing an efficient control on the power flow [3]. Several control strategies have been tested on each device so that we can select the most efficient one. We have tried to link the results with the observability rescaled [4] as well as concerning the physical origin of the oscillations. The position of the devices is also taken into account during the discussions.

The paper is organized as follows. In section 2 system modeling and SIME model are introduced. Section 3 describes the FACTs devices. Different control strategies are discussed in section 4. Section 5 deals with application of these control strategies to test power system, the results and the discussion of the results at the same time. We eventually end up with the conclusion.

2 SYSTEM MODELING

An electrical network of Multi-Machine Power System (MMPS) is a non-linear system described by following non-linear state equations of the form:

$$\dot{x} = f(x, y, u)$$
$$0 = g(x, y, u) \qquad (1)$$

where, x is a vector of state variables related with the dynamic of generators, loads and other system controllers. y is a vector of algebraic variables related with voltage phasors , u is a vector of input variables. Here f describes power generation dynamics of MMPS.

For a large interconnected power system, inter-area oscillation is one of the major concerns for stability analysis. In inter-area oscillation, kinetic energy is exchanged within remote groups of generators. The frequencies of inter-area oscillations are typically in the range of 0.2 Hz to 0.8 Hz [3]. Poorly damped inter-area oscillations become more pronounced in risking system stability when fault occurs into the system. The purpose of faults is to stress the Power Oscillations (PO). The nature of the disturbance will define the kind of mode that can be stressed. A disturbance in the power consumption efficiently affects the inter-area modes of oscillation. The location of the disturbance will stress one specific mode as long as it is between oscillating generator groups. The target is to damp the inter-area oscillations to have more robust network. Controllable components like FACTs devices and VSC-HVDC came out as a solution to increase system stability margin. These components are also able to damp inter-area oscillation. Different control techniques can be implemented on different controllable components to improve power oscillation damping.

In order to analyze and compare the effect of different control strategies of controllable components used in MMPS, Single Machine Equivalent Method (SIME) model is used. SIME method assesses post-fault configuration of MMPS by replacing the trajectories of MMPS with a trajectory of a one machine infinite bus system of following form:

- *Aziz Un Nur Ibn Saif is a Lecturer in the Dept. of Electrical and Electronic Engineering in Ahsanullah University of Science and Technology, Bangladesh, E-mail: aziznur.saif@gmail.com*
- *Md. Masum Howlader is pursuing masters degree in Institute of Electric Power Systems and High-voltage Technology in Kurlshrue Institute of Technology, Germany, E-mail: uodql@student.kit.edu*
- *Md. Tareq Ul Islam is currently pursuing masters degree program in the Dept. of Electrical Engineering in Eindhoven University of Technology, The Netherlands, E-mail: m.tareq.ul.islam@student.tue.nl*

$$\dot{\delta}_{SIME} = \omega_{SIME}$$
$$\dot{\omega}_{SIME} = M^{-1}\left[P_{mSIME} - P_{eSIME}\right] \quad (2)$$

where, P_{mSIME} and P_{eSIME} are respectively the equivalent mechanical input power and the equivalent electrical output power.

After subjecting the power system with disturbances which supposedly leads the system to instability and using time domain program, the mode of instability is identified where machines are separated into two groups: i.e. critical machines (subscript C) and non-critical machines (subscript NC). In this paper these two groups are formed by the two groups of generators involved in inter-area oscillation. Now this two-machine equivalent is replaced by a single machine equivalent system [4,6]. The SIME parameters are rotor angle (δ), rotor speed (ω). The parameters of (2) are

$$\delta_{SIME} = \delta_C - \delta_{NC} \quad (3)$$
$$\omega_{SIME} = \omega_C - \omega_{NC} \quad (4)$$

where, $\delta_{C/NC}$, $\omega_{C/NC}$ are respectively the average of the rotor phase deviation and speed deviation weighted by the inertia constant M_i of each generator [6].

3 Controllable Components

This section briefly describes the basic structure of the controllable components used in this project:

2.1 SVC

Static Var Compensators (SVCs) are normally utilized in order to control the bus voltage to a reference value. SVC usually includes a thyristor controlled reactor (TCR) to consume reactive power when voltage goes beyond reference and thyristor switched shunt capacitor / fixed shunt capacitor bank rated for maximum capacitive power required Fig. 1(a). It is connected in shunt at the bus which requires mainly voltage control. Hence in principle SVC is a controlled shunt susceptence.

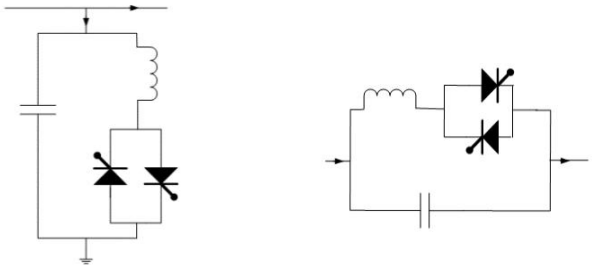

(a) (b)

Fig. 1. Basic Structure of SVC (a) and TCSC (b)

2.2 TCSC

A TCSC is connected in series with the transmission line and can be considered as controllable capacitive reactance. The basic configuration of TCSC Figure 1(b) usually is a fixed capacitor (FC) in parallel with a Thyristor Controlled Rectifier (TCR). The reactance of this whole arrangement can now be modulated within a certain range by means of controlling the firing angle of the thyristors which is eventually utilized as a tool of changing power flow on parallel transmission lines. This results the improvement of transient and voltage stability of system.

2.3 VSC-HVDC

The VSC-HVDC system connects two ac systems with a HVDC link as depicted in Fig. 2. The VSC converters at both ends of the HVDC line can generate ac voltage with any phase angle or voltage amplitude within certain limits using Pulse Width Modulation (PWM) technique.

Two converter stations residing at terminal ends of HVDC line provides the opportunity to control both active and reactive power separately. The active power or dc side voltage is regulated using the set point of active power loop. Similarly the reactive power control loop is used to apply controlling of either the reactive power or ac side voltage. Two modes explained so far can be chosen autonomously at either end of HVDC line [5].Every component can control the power transmitted through its bus or line [5][6][8]. This is the reason why they can damp the PO.

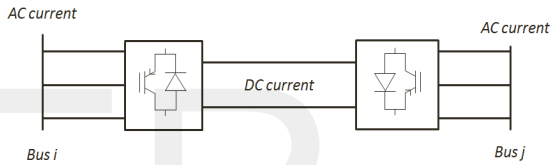

Fig. 2. Basic Structure of VSC-HVDC

4 Control Techniques

The focus of this paper is to devise different control strategies for Power Oscillation Damping (POD) controller that will be implemented in above mentioned controllable components. The dynamic model of controllable components consists of three parts: PI regulator, POD and Time delay. The PI regulator measures one of the parameter from the system, compares it with reference value and modulates control variable associated with the component. The time delay represents the delay induced by the device [9]. The POD will control the damping of the inter-area mode. Four strategies are implemented. Basically two are linear control strategies based on modal analysis and the two are non-linear control strategy based on Control Lyapunov Function (CLF).

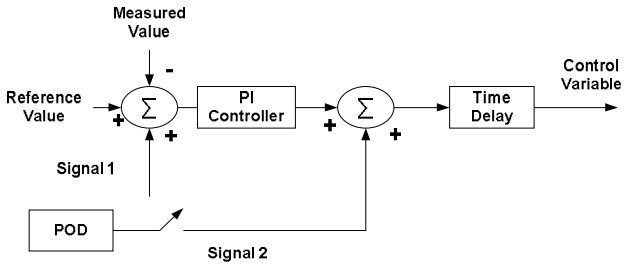

Fig. 3. Simple dynamic model of controllable components

4.1 Modal Analysis Method [10]

By linearizing the power system dynamics of (1) around an equilibrium point, we obtain the following equations:

$$\Delta\dot{x} = A\Delta x + B\Delta u$$
$$\Delta\dot{Y} = C\Delta x + D\Delta u \qquad (5)$$

where, A is the state matrix, B is the input matrix, C the output matrix and D is the feed forward matrix. Δx is the state vector, Δy is the output vector and Δu is the input vector. The matrices of the open loop transfer function of (8) are obtained for a particular input and output variables using software of simulation (SIMPOW) [11]. A feedback controller (regulator) is utilized to close the control loop. In the controller designing approach that discussed in this report, forward transfer function G(s) represents power system with FACTs device and feedback transfer function represents POD controller.

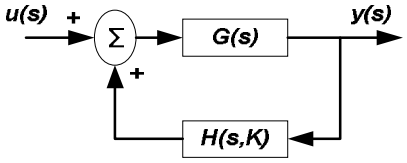

Fig. 4. Closed loop system with POD controller

An eigen-analysis of matrix A results in the eigen-values λ_i and corresponding matrices of right and left eigen-vectors V^r and V^l respectively. Each eigen-values λ_i is associated with a mode of the system. The transfer function of open loop system is expressed by,

$$G(s) = \sum_{i=1}^{n} \frac{R_i}{(s-\lambda_i)} \qquad (6)$$

where R_i is the residues matrix associated with inter-area mode λ_i. A residue of $G(s)$ associated with inter-area mode (i-th) is introduced (9) in order to calculate the parameters of the linear controller,

$$R_i = CV_i^r V_i^l B \qquad (7)$$

In order to alter a particular mode of a system with signal coming from feedback controller (POD controller), it is necessary that its k[th] input signal $u_k(t)$ affects the state of the ith mode $\zeta_i(t)$ and that its j[th] output signal $y_j(t)$ is correlated with $\zeta_i(t)$. These two properties can respectively be evaluated by modal controllability $C_{i,k}$ and observability, $O_{i,j}$.

$$y_j(t) = \sum O_{i,j}\zeta_i(t) \qquad (8)$$

$$\zeta_i(t) = \lambda_i\zeta_i(t) + \sum C_{i,k}u_k(t) \qquad (9)$$

In order to compare $O_{i,j}$ for different j and $C_{i,k}$ for different k it is necessary to rescale these values. The rescaled values $O_{i,j,resc}$ and $C_{i,k,resc}$ are given by the formulas introduced by [4]. Due to the addition of feedback system, $H(s,K) = KH(s)$ the change of ith mode (inter-area mode) is:

$$\Delta\lambda_i = R_i KH(\lambda_i) \qquad (10)$$

The structure of the linear POD (LELA) that is used in this paper is shown in Fig. 5.

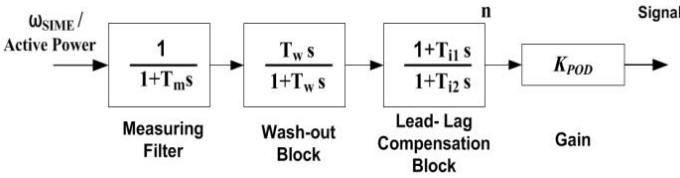

Fig. 5 POD controller [7]

The first block is measuring filter (low pass filter), then washout block (high pass filter). The purpose of the washout block is to stop contribution from steady state input deviation. After that lead-lag compensation blocks (n=no of stages) are introduced to phase shift of the input signal by varying its parameter T_{i1} and T_{i2} in such a way that a positive contribution to damping is obtained. At last, gain is introduced to determine the magnitude of damping provided by POD. The transfer function $H(s)$ of POD controller can be expressed as,

$$H(s,K) = K_{POD}\left[\frac{1}{1+T_m s}\right]\left[\frac{T_w s}{1+T_w s}\right]\left[\frac{1+T_{i1}}{1+T_{i2}}\right]^n \qquad (11)$$

T_{i1} and T_{i2} are lead, lag time constant respectively determined by,

$$T_{i2} = \alpha T_{i1}, \qquad T_{i1} = \frac{1}{\omega_i\sqrt{\alpha}} \qquad \alpha = \frac{1-\sin(\varphi/n)}{1+\sin(\varphi/n)}$$

T_{i1} and T_{i2} the compensation angle, $\varphi = \pm 180° - \arg(R_i)$. Note that the sign of $\pm 180°$ is the same has the sign of the imaginary part of the residue.

The target is to tune T_{i1} , T_{i2} and K_{POD} to phase shift the residue of the inter-area mode to the negative axis and make real component of $\Delta\lambda_i$ more negative to improve damping as depicted in Fig. 6. An input and an output have to be selected to drive the POD. The output is signal 1 regarding the Fig. 3. The input must give relevant information about the power oscillation, which is the case for both ω_{SIME} and active power flowing from the C to the NC machines regarding (2).

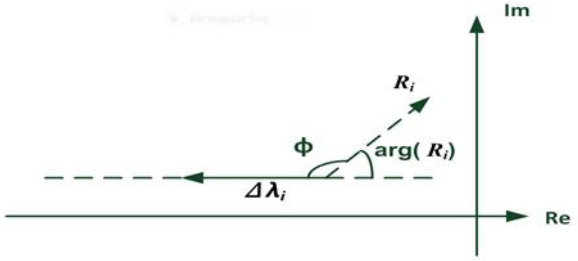

Fig. 6 Phase shift of residue

4.2 CLF Method [12]

Lyapunov theorem usually applies for closed loop system since it only deals with dynamically system without input. Control Lyapunov Function (CLF) is introduced to find the existence of a feedback control $u = u(x)$ that will make the closed loop system with control input such as

$\dot{x} = f\left(x, u\left(x\right)\right)$ asymptotically stable around an equilibrium point, x_0 i.e. $f\left(x_0, u\left(x_0\right)\right) = 0$. If the existence of previous described control input $u\left(x\right)$ is found, then the function $u\left(x\right)$ is termed as stabilizer. A stabilizer is expressed as,

$$u\left(x\right) = -grad\left(\upsilon\right).f\left(x\right) \qquad (12)$$

where, $\upsilon\left(x\right)$ is the Control Lyapunov Function (CLF) satisfying all necessary conditions [12].

It can be mentioned that the existence of CLF is necessary and sufficient to ensure stability of a system with control input. On the other hand, existence of Lyapunov function is necessary and sufficient to stabilize a system without control input. Applying CLF based control law in the controllable components described in section II for MMPS we get the same expression of the POD CLF for every device,

$$signal_{1/2} = K_{POD} sin\left(\delta_{SIME}\right)\omega_{SIME} \qquad (13)$$

5 Simulation and Results

5.1 General description of the system

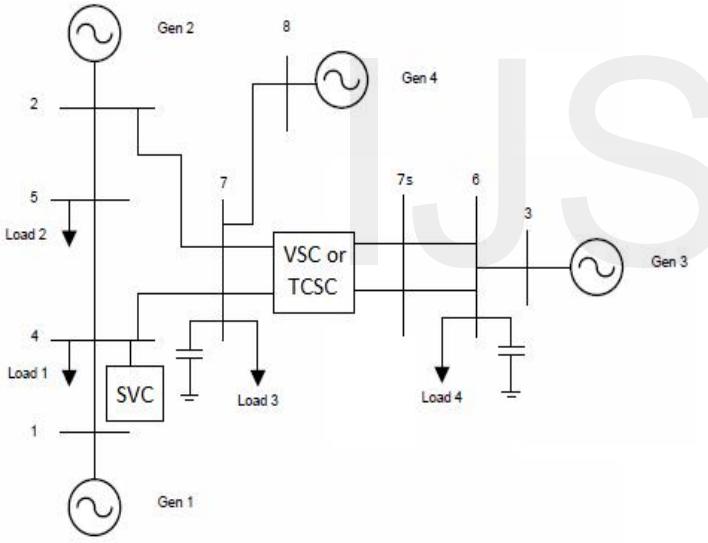

Fig. 7 Test system including location of three FACTS & HVDC devices which will be implemented individually.

There are both a static and a dynamic simulation. Fig. 7 is a representation of the static description where the four generators are implemented according the two axis-model, the four loads are modeled as power loads and the short line model is in used [1]. Table 1 gives some of the parameters in use. The result of the power flow analysis shows that the SVC establishes thus bus voltages closer to their nominal values than the other devices. The modal analysis Fig. 8 claims that the less damped PO is induced by the generator 3 oscillating against the generators 1, 2, 4. A similar consideration shows that the second less damped mode is induced by the generator one oscillating against the generator 2.

TABLE 1: APPARENT POWER S AND POWER FACTOR $\cos\varphi$ OF THE LOADS AND CLASSICAL MODEL PARAMETERS OF GENERATORS

Load nb	S [MVAR]	$\cos\varphi$	Generator nb	M_i[Nm.s]	Sn[MVAR]
1	602	0,997	**1**	12000	1200
2	170	0,999	**2**	12000	1200
3	1202	0,998	**3**	14400	1200
4	150	0,998	**4**	5000	500

About the dynamic simulations, two different faults are selected. One is larger than the other: a three phase fault to the ground at a bus 3 and a temporary 5% decrease of the load 3. Fig. 11(a), (c), (e) shows that the large fault strongly stresses the inter-area mode. Indeed, the temporary grounding of bus3 raises the kinetic energy of generator 3 but not of the others. Thus, once the fault is cleared, the extra kinetic energy oscillates between the generator 3 and the generators 1, 2, 4. Fig. 11(b), (d), (f) shows that the small disturbance affects several mode. Indeed, the load 3 is the largest one and is fed by every generator according to a power flow analysis [1]. Thus its sudden reduction will induce an increase of the kinetic energy of every generator which will be released and will stress every PO at the same time.

The Software called SIMPOW [11] is used in order to get the simulations results regarding the network Fig. 7 and the two faults. It can run the power flow, can give the modal analysis, the ABCD matrix and can simulate the time behavior of the system after the faults. The behavior of our interest is the power oscillation (PO) between the critical and non-critical generators. We know from section I that δ_{SIME} shows the PO. Thus the figures representing $\delta_{SIME}\left(t\right)$ will determine the actual damping of the interarea mode after applying each of the faults.

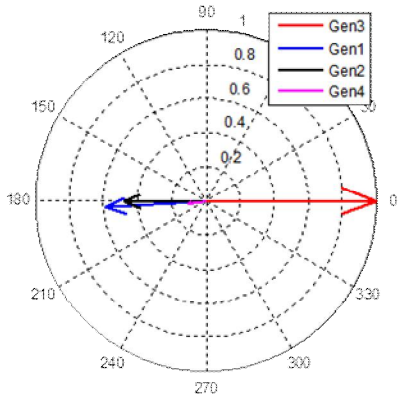

Fig. 8 Phasor diagram of kinetic energy [pu]. The energy in generator 3 is maximal when the others is minimal.

We know also that the power transmission between the two groups of generators is relevant information to command the POD. Thus the power flowing from bus 3 to bus 6, $P_{3,6}$ is relevant while the power flowing from bus 1 to 4 is less relevant. The linear POD of the TCSC controller is commanded by $P_{3,6}$ while $P_{1,4}$ commands SVC's. Accordingly

the first case should be more specific to damp the selected inter-area mode. A specific POD is a controller which can damp the selected mode without altering the other modes. For instance Fig. 9 shows that the LELA with the power as input (LELA_mw) is more specific than the CLF control when implemented on the TCSC. This is due to the facts that the CLF control inputs, ω_{SIME} and δ_{SIME} are more sensible to the mode whose frequency is 0.85Hz ($\omega = 5.2\ rad.s^{-1}$) than $P_{3,6}$. Indeed this other mode corresponds to a PO between the generators 1 and 2. $P_{3,6}$ is independent from this PO regarding its location while the SIME variables are function of the rotor phase angle of generator 1 and 2. However, regarding TABLE 1 these two generators are very similar, and their rotor phase angles are actually added in (3) thus the oscillation between both should cancel out in the expression of the SIME variables (3). That is why the CLF implemented on a TSCS can still be considered as being specific.

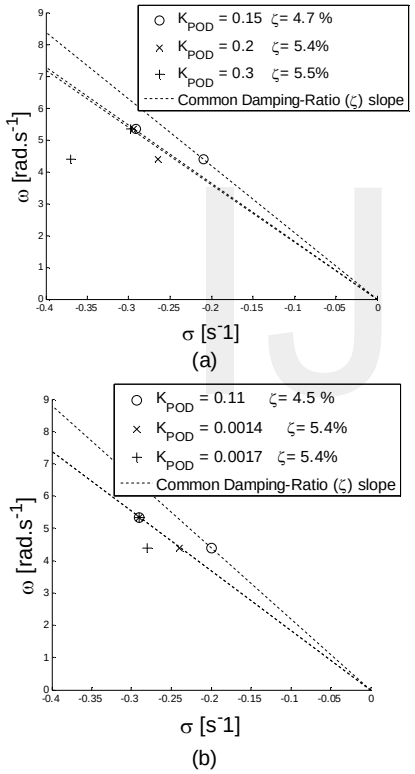

Fig. 9 Evolution of two lowest damped modes for 3 different K_{POD} when POD CLF (a) and LELA_mw (b) are implemented on the TCSC

On the other hand, when the CLF is implemented on the SVC, it is not specific any longer (Fig. 10). The reason is not linked with the input of the POD anymore but should rather be found considering the location of the device. Since it is located between the C and NC of the second lowest damped mode, it does have an impact on this PO no matter what the POD strategy is. However this impact can be either improve the other lowest damped modes Fig. 10(a) or deteriorate it Fig. 10(b). In the first case we have been limited by the change of direction of the eigenvalue (residue) but in the second case it is the second less damped mode which becomes the less damped mode for a too high gain of the POD.

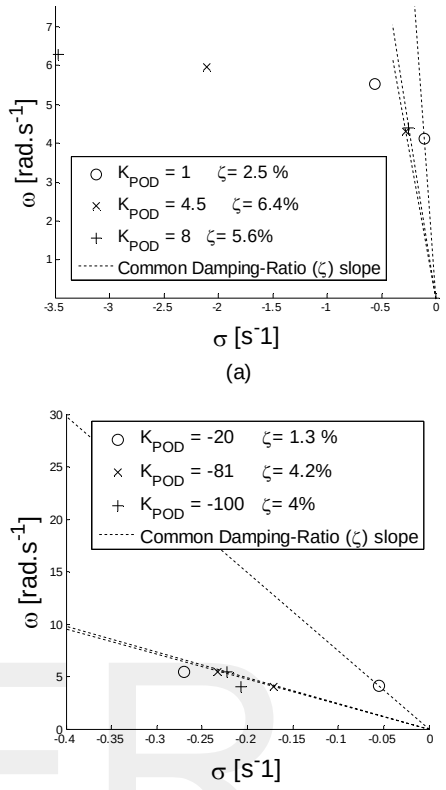

Fig. 10 Evolution of the two lowest damped modes for 3 different K_{POD} when POD CLF (a) and LELA_mw (b) are implemented on the SVC

Finally, the specificity of a POD is both function of the input and the location of the device that it controls. Moreover, if the location of the device makes the specificity impossible, such as the SVC case, an appropriate choice of input can turn this non-specific feature to our advantage. And if the POD is specific, we could decide to deeply damp the former inter-area mode without altering the other modes two much. Similarly to the cases shown as example we have computed the gain of our POD so that the damping ratio of the less damped mode is maximal. By doing so, the gain is often obtained when the less and the second less damped modes have the same damping ratio except at case Fig. 10(a) where the optimal gain is obtained when the direction of the less damped mode changes. For a given device, the gain is different depending on the POD while the obtained damping ratio is the same. This is mainly respectively related to the observability and controllability of the inputs and output of the POD. Indeed TABLE 2 shows that the higher product $C_{i,k,resc} * O_{i,j,resc}$, the lower the gain. A look at (10) makes it understandable knowing that the product is similar to the residue R_i (7). For instance (8) shows that for a given variation of $\zeta(t)$, $y_j(t)$ varies less if $O_{i,j}$ is smaller. In order to compensate this lack of variation, a larger gain is required.

TABLE 2: OBSERVABILITY, CONTROLABILITY AND GAIN OF EACH POD

Device	$C_{i,k,resc}$ [%]	Input of LELA	$O_{i,j,resc}$ [%]	K_{POD}
SVC	0.0305	ω_{SIME}	0.56	48
		$P_{1,4}$	8.45	4.5
TCSC	0.495	ω_{SIME}	0.69	5
		$P_{3,6}$	6.35	0.0014

Moreover for a given device, the optimal damping ratio is the same for each POD regulator except LELA_mw on SVC. Those similarities are shown Fig. 11. There are at least two other observations concerning Fig. 11. First, Fig. 11(b) shows that the SVC implemented with a POD whose input is $P_{1,4}$ damps faster the PO while subjected to a large disturbance than subjected to a small disturbance. An explanation could be that the disturbance has caused a relatively larger change on $P_{1,4}$ during the small disturbance than during the large one whereas its change is not only related to the considered PO, but also to the PO between generator 1 and 2. The problem relies in the fact that this useless deviation will still drive the POD while this deviation is not correlated to the PO in purpose. But once the first swing ends, the wrong PO has been damped so $P_{1,4}$ gets fully correlated to the PO in purpose. The damping ratio gets larger because at t=15s, the PO is more damped with the power POD (blue curve) than with the other POD. The change of frequency at the Fig. 11(b) confirms the change of frequency observed Fig. 10(a). Finally, Fig. 11(e), (f) shows that the damping maximal minimal damping is the same no matter where the POD signal is applied but its gain has to 10 times higher when applied at signal 2 than signal 1. The reason is that the signal 1 gets profit of the gain of the PI controller while signal 2 cannot because it is applied after the PI controller Fig. 3. Since we prefer lower gains, the first signal is in used for every simulation. Indeed a lower gain should cost less.

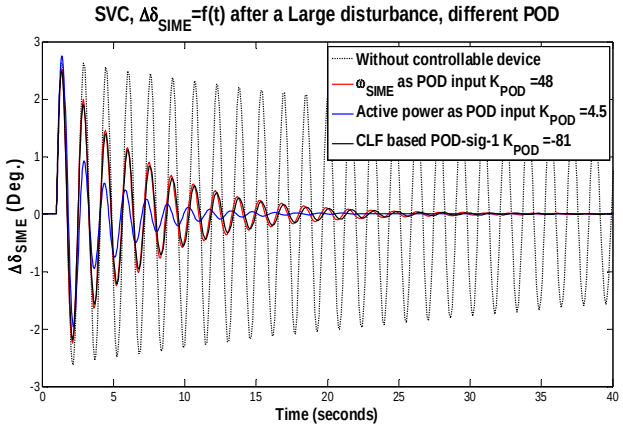

(a)

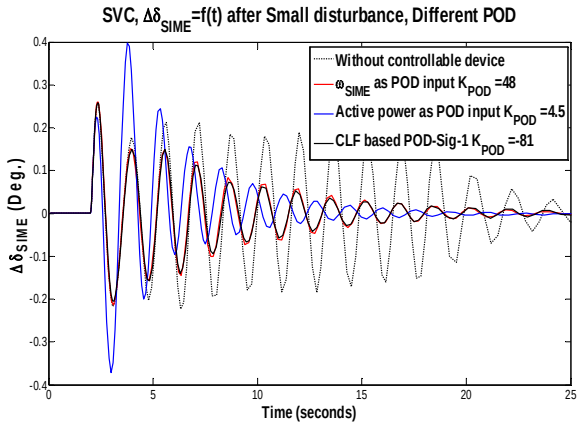

(b)

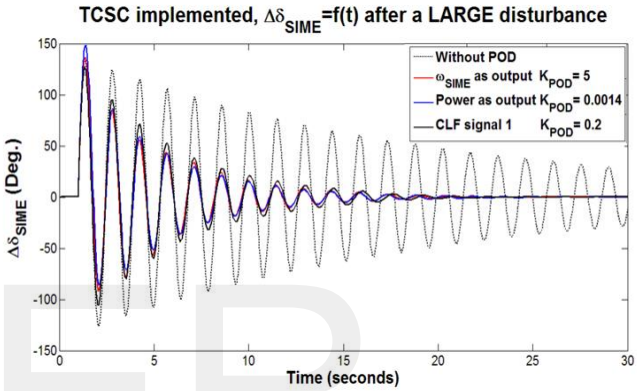

(c)

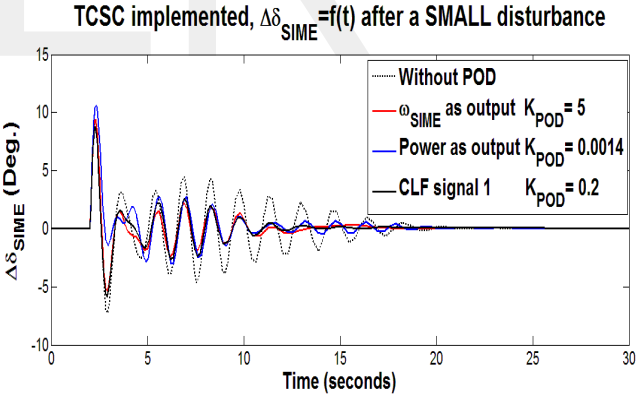

(d)

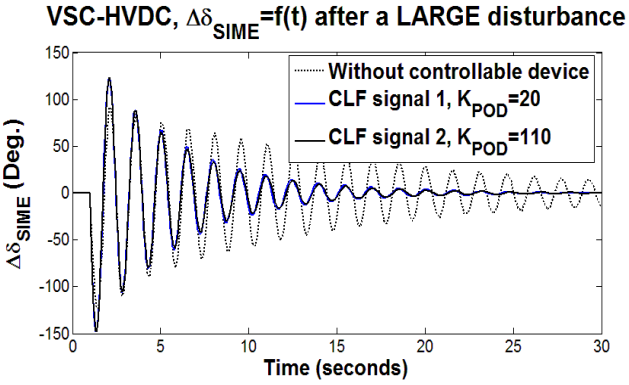

(e)

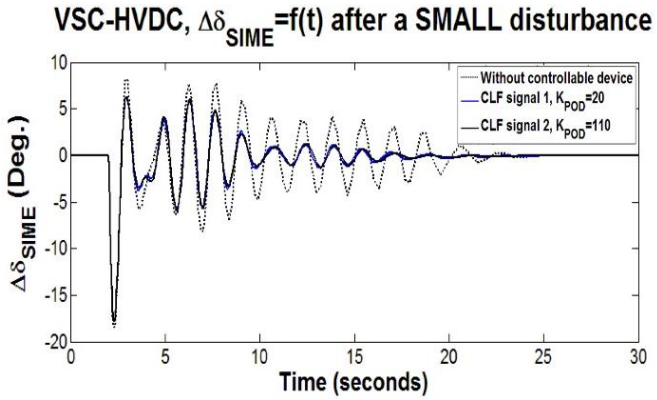

(f)

Fig. 11 $\Delta\delta_{SIME} = f(t)$ for every device, every POD tuned such as the minimal damping ratio is maximal.

6 Conclusion

The FACTS and HVDC devices have an impact on the voltage at steady state and the PO when a POD is implemented. The SVC enhances the bus voltages closer to their nominal value. The nature of their POD and their location are relevant factor to define the impact on the PO. Since each combination has pro and con, the operator has to define his objective. If the objective is to get rid of one power oscillation, a specific POD is required; for instance the lead-lag filter with the power as input is the best specific control when implemented on a TCSC located between the critical and non-critical generators. If the aim is to reduce the minimal damping ratio, the SVC located between some C and some NC generators of the two less damped PO will be a reasonable choice. But the designer still has to test several POD strategies because our simulations haven't highlighted a better general strategy. To finish with, the advantage to select the output variables with the best observability is to limit the gain of the POD.

References

[1] Kundur, P., *Power System Stability and Control* (McGraw-Hill Inc., 1994).
[2] Kirschner, L., Retzmann, D.,Thumm, G., *Benefits of FACTS for Power System Enhancement*, Transmission and Distribution Conference and Exhibition, Asia Pacific, 2005.
[3] Bachmann, U., Berger, F., Reinisch, R.: *Possibilities of Multifunctional FACTs Application in the European Electric Power System under the Changing Conditions of the Liberized Electricity Market*, CIGRE (Germany), 2002.
[4] Hamdan, A. M. A., Elabdalla, Geometric Measures of Controllability and Observability of Power System Models, Electric Power System Reasearch, March 1988, pp.147-155.
[5] Bahrman MP, Johnson BK. The abcs of hvdc transmission technologies. IEEE Power & Energy 2007; 5(2):34–35, 44.
[6] Ghandhari, M., Andersson, G., Pavella, M., Ernst, D.: *A Control Startegy for controllable series capacitor in electric power systems*, Automatica 37, 2001, pp. 1575-1583.
[7] Latorre, H. F., Ghandhari, M.: *Improvement of Power System Stability by using VSC-HVDC*, Electrical Power and Energy Systems, Elsevier 33, 2001, pp. 332-339.
[8] Einer, E., Mi ller, N., Nilsson, S.: *Benefits of GTO based compensation systems for electric utility applications*, IEEE Transactions on Power Delivery, Vol. 7, No. 4, October 1992.
[9] *Modeling of Power Electronics Equipment in Load flow and Stability Programs*, Task Force 38.01.08, CIGRE, August 1999.
[10] Yang, N., L iu, Q., McCally J. D .: *TCSC Controller Design for Damping Inter-area Oscillation,* IEEE Transactions on Power Systems. Vol. 13, No. 4, November 1998.
[11] SIMPOW®, *User manuel,* 11.0 Ed., 2010.
[12] Ghandhari, M., Andersson, G.: *Control Lyapunov Functions for Controllable Series Devices*, IEEE Transactions on Power Systems. Vol. 16, No. 4, 2001.